518 Transaction of the Korean Society of Mechanical Engineers, Vol. 9, No. 4, pp. 518~527, 1985.

<**Original**>

Natural Convection in a Rectangular Cavity Washed Externally by a Turbulent Boundary Layer

Chul-Jin Choi* and Keun-Shik Chang*

(Received April 30, 1985)

外部 亂流 境界層과 結合된 직사각형 空洞에서의 自然對流

최 철 진 · 장 근 식

Key Words: Natural Convection(자연대류), Turbulent Boundary Layer(난류경계층), Conjugate Heat Transfer (복합열전달), Rectangular Cavity (직사각형 空洞), Finite Difference Methods(유한차분법)

초 록

대류-대류의 복합 열전달 문제를 유한차분법을 사용하여 수치적으로 연구하였다. 아래로 부터 가열되는 직사각형 공동 내에서의 자연 대류와 공동 위쪽의 외부 난류 경계층 유동이 복합된 경우의 열전달 현상을 고려하였다. 두개의 서로 다른 모우드의 대류가 온도 분포가 미리 알려져 있지 않은 얇은 수평평판에 의해 분리되어져 있다는 점이 본 논문의 특이점이다.

수치적 해석은 Reynolds 수와 Grashof 수 및 공동의 기하학적 종횡비의 매개 변수적 효과가 발견되도록 행하여 졌다. 외부 난류 경계층 유동의 강도에 따라 공동 내에서의 유동 형태가 변할 수 있음을 알았다. 즉 내부 부력 세포의 회전 방향은 외부 유동의 존재에 의해 특성적으로 정해지며 공동 내의 유동 세포의 수는 Grashof 수가 증가 할수록 많아진다.

Nomenclature

A : Aspect ratio, H/L

g : Gravitational acceleration

Gr_L : Grashof number based on L, $g\beta L^3(T_h-T_f)/\nu^2$

Gr_H : Grashof number based on H, $g\beta H^3(T_h-T_f)/\nu^2$

H : Vertical depth of a rectangular cavity

J : Heat equivalent of mechanical work

L : Horizontal width of a rectangular cavity

Pr : Prandtl number, ν/α

p : Pressure

Q : Overall rate of heat transfer

Re_f : Reynolds number, $U_f L/\nu$

t' : Dimensional time

T : Temperature

u', v' : Dimensional velocity components in (x', y') coordinates or velocity fluctuations

U, V : Mean velocity components in the external boundary layer

x', y' : Cartersian coordinates, dimensional

X, Y : Computational coordinates

ΔX : Mesh size in the X-direction

* Member, Department of Mechanical Engineering, Korea Advanced Institute of Science and Technology

Subscripts

h : Hot
f : Freestream
w : Interface wall

Superscripts

$'$: Ttrbulent fluctuation or dimensional quantity
$*$: Stagnation

1. Introduction

Coupling of natural convection to forced convection heat transfer through a diathermal partition is a common occurence in our technical environment. The solar energy collector devices, heat exchangers and house window panes are just a few examples among the many important applications. In the present paper, a model problem is constructed to study one of such conjugate heat transfer applications: natural convection in a rectangular cavity coupled with an external turbulent boundary layer. Heat transfer from a double window pane in a cold windy day could be envisioned by this problem.

Mathematically, such a problem poses tremendous difficulty due to the many parameters involved, nonlinearity, unknown thermal condition at the interface, and the different heat transfer modes in the internal and external fluids. Nevertheless, an approximate solution to such a conjugate heat transfer is accessible by means of numerical methods geared for the high speed digital computer. Matching the cavity flow with the external boundary layer can be achieved through the requirement of heat flux continuity at the partition, whose thickness is assumed infinitely thin for simplicity.

Rectangular cavity problem has received intensive attention in the literature. When a layer of fluid is heated uniformly from below, cellular convection is generated. When the Grashof number is raised above a certain critical value, the motion which remains laminar and steady for a large of Grashof number turns into unsteady and turbulent convection. This cavity flow has been studied by many authors after Benard(1~9). Deardorff(4) used finite difference techniques to approximately integrate the Navier-Stokes equations. Length-to-height ratios 1 and 2, and Rayleigh numbers greater than 6.75×10^5 were considered. In most cases he obtained a nearly steady solution. Fromm(5) investigated a fluid layer heated from below for the Rayleigh number ranging up to 10^7. Other numerical investigation was made by Küblbeck *et. al.*(6). They have constructed a two dimensional, time dependent numerical method for the laminar free convection in a closed cavity. More recently, heat loss in the inclined rectangular cavity has recieved considerable attention by designers of solar collector(7~9).

The convection-to-convection conjugate heat transfer as the present problem has been little considered in the literature. Lock and Ko(12) have performed a numerical study on the problem of two reservoirs in different temperature, seperated by a vertical flat plate with a piece of diathermal window in the middle. The coupled buoyant boundary layers developing along the both sides of the partition, one in opposite direction to the other, are solved numerically by an iterative process. In the present paper, the thermal energy delivered by the Navier-Stokes flow in the cavity is taken away on the top by an external forced convection.

2. Cavity Flow

We consider a closed two dimensional cavity of length L and height H which contains a Newtonian fluid; see Fig. 1. The vertical side walls are insulated and the bottom is held at a uniform temperature T_h. The top is exposed externally to a forced convection whose free stream velocity and temperature are U_f and $T_f(<T_h)$, respectively. The hydraulic boundary layer has leading distance D ahead of the thermal boundary layer.

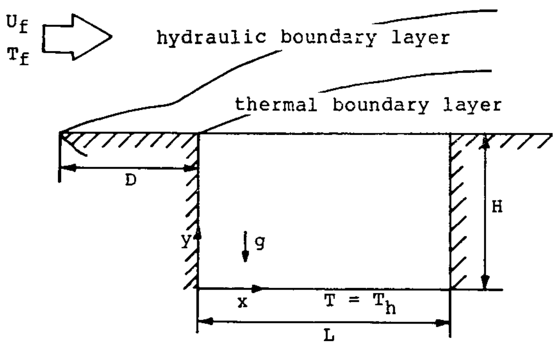

Fig. 1 Externally blown rectangular cavity

2.1. Governing Equations

The problem under consideration is assumed two dimensional, steady and laminar, Due to the intractability of the full Navier-Stokes equations for the buoyant viscous flow, we adopt the Boussinesq approximation as usual. We denote the kinematic viscosity, density, thermal diffusivity and thermal expansion coefficient, all referred to some constant temperature in the flow system, as ν, ρ, α and β, respectively. Nondimensional variables are introduced as follows:

Length $\quad x=x'/H,\ y=y'/H \quad (1)$

velocity
$$u=\frac{u'}{g\beta H^3(T_h-T_f)/\nu L} \quad (2)$$
$$v=\frac{v'}{g\beta H^3(T_h-T_f)/\nu L}$$

temperature
$$\theta=\frac{T-T_f}{T_h-T_f} \quad (3)$$

time
$$t=\frac{t' g\beta H^2(T_h-T_f)}{\nu L} \quad (4)$$

vorticity
$$\zeta=\frac{\dfrac{\partial v'}{\partial x'}-\dfrac{\partial u'}{\partial y'}}{g\beta H^3(T_h-T_f)/\nu LH} \quad (5)$$

Then, the governing equations becomes nondimensionally

$$Gr_H A^2\left(\frac{\partial \zeta}{\partial t}+u\frac{\partial \zeta}{\partial x}+v\frac{\partial \zeta}{\partial y}\right)=A\nabla^2\zeta+\frac{\partial \theta}{\partial x} \quad (6)$$

$$Gr_H Pr A\left(\frac{\partial \theta}{\partial t}+u\frac{\partial \theta}{\partial x}+v\frac{\partial \theta}{\partial y}\right)=\nabla^2\theta \quad (7)$$

$$\zeta=-\nabla^2\psi \quad (8)$$

where, $\quad u=\dfrac{\partial \psi}{\partial y},\quad v=-\dfrac{\partial \psi}{\partial x}$

The boundary conditions are, in a steady state,

$$\begin{aligned}
&\psi=0,\ \frac{\partial \psi}{\partial x}=0 && \text{at } x=0,\ 1/A, && 0\le y\le 1\\
&\psi=0,\ \frac{\partial \psi}{\partial y}=0 && \text{at } y=0,1, && 0\le x\le 1/A\\
&\frac{\partial \theta}{\partial x}=0 && \text{at } x=0,1/A, && 0\le y\le 1 \quad (9)\\
&\theta=1 && \text{at } y=0, && 0\le x\le 1/A\\
&\theta=f(x) && \text{at } y=1, && 0\le x\le 1/A
\end{aligned}$$

It is noted that the function $f(x)$ is unknown *a priori*, subject to the condition $f(0)=0$ and $0\le f(x)\le 1$. Although the characteristic velocity scaling might at first appear to be an arbitrary choice, it is consistent with the physical nature of the buoyancy-driven cavity flow as was justified by Cormack *et. al.*(13).

2.2. Numerical Formulation

Before performing the finite difference approximation, we make coordinate stretching in y-direction to cluster more mesh points toward the horizontal interface partition. This is necessary to accurately account for the sharp gradients of the flow properties in this region. We choose the transformation relations $X=Ax$ in the x-direction, and in the y-direction

$$Y(y,\varepsilon)=\frac{\tan\left(\frac{\pi}{2}\varepsilon y\right)}{\tan\left(\frac{\pi}{2}\varepsilon\right)} \tag{10}$$

Here, the deformation parameter ε is determined from the ratio of heighty to width of the cavity.

The governing equations and boundary conditions are now cast to the finite difference form. The successive line over relaxation method is used to solve the resultant finite difference equtions. In this approach, the governing equations are discretized by basically using a central differencing technique. The nonlinear convective terms cause main difficulty in achieving numerical stability. It can be overcome by using the second upwind differencing scheme as tried by Lilly[14]. Sample demonstration is

$$\left(u\frac{\delta v}{\delta X}\right)_{i,j}=\{(u_R-|u_R|)v_{i+1,j} + (u_R+|u_R|-u_L+|u_L|)v_{i,j} - (u_L+|u_L|)v_{i-1,j}\}/(2\Delta X) \tag{11}$$

where, $u_R=(u_{i+1,j}+u_{i,j})/2$,

$u_L=(u_{i,j}+u_{i-1,j})/2$

The second-order derivatives in the diffusion term and the non-convective first-order derivative term, which are a consequence of the coordinate transformation as well as the buoyancy term, are approximated by the centered space approximation. Substituting these approximations into the transformed governing equtions, one obtains the tridiagonal matrix systems. We solve these systems by Thomas algorithm.

3. Turbulent Boundary Layer

The two-dimensional turbulent steady forced convection over a flat plate is mathematically governed by the time-averaged continuity, momentum and energy equations. There exist excellent numerical methods as given by Patankar and Spalding[20], and Crawford and Kays[11]. The latter authors write the governing equations as

$$\frac{\partial U}{\partial x}+\frac{\partial V}{\partial y}=0 \tag{13}$$

$$U\frac{\partial U}{\partial x}+V\frac{\partial U}{\partial y}=\frac{1}{\rho}\frac{\partial}{\partial y}\left(\frac{\partial U}{\partial y} - \overline{\rho u'v'}\right) \tag{14}$$

$$U\frac{\partial I^*}{\partial x}+V\frac{\partial I^*}{\partial y}=\frac{1}{\rho}\frac{\partial}{\partial y}\left(\frac{k}{c}\frac{\partial I}{\partial y} - \overline{i^{*\prime}v'}+\frac{\mu}{J}\frac{\partial}{\partial y}\left(\frac{U^2}{2}\right)\right) \tag{15}$$

where I^* is the stagnation enthalpy of the fluid defined by $I^*=I_f+U^2/2J$, and I is the static entalphy. In the momentum equation, the turbulent shear stress $\overline{-u'v'}$ is modeled using the eddy diffusivity ε_m defined by

$$\overline{-u'v'}=\varepsilon_m\frac{\partial U}{\partial y}=\frac{\mu_t}{\rho}\frac{\partial U}{\partial y} \tag{16}$$

where μ_t is the turbulent viscosity.

In the energy equation, the term $\overline{-i^{*\prime}v'}$ is a correlation involving the fluctuation of the stagnation enthalpy and the cross-stream velocity, and is approximated as

$$\overline{-i^{*\prime}v'}=\overline{-i'v'}+U(\overline{-u'v'}) \tag{17}$$

where i' is the fluctuation of the static enthalpy. The turbulent heat flux $\overline{-i'v'}$ is modeled using the eddy diffusivity for heat, ε_h, defined by

$$\overline{-i'v'}=\varepsilon_h\frac{\partial I}{\partial y}=\left(\frac{k_t/c}{\rho}\right)\frac{\partial I}{\partial y} \tag{18}$$

where k_t is the turbulent conductivity.

For the boundary layer in the present problem consisting of a wall and a freestream, the kinematic boundary conditions are given by

$$U(x,0)=V(x,0)=0 \tag{19}$$

$$\lim_{y\to\infty} U(x,y)=U_f$$

The thermal boundary conditions are

$$\dot{q}(x,0)=-\frac{k}{c}\frac{\partial I^*(x,0)}{\partial y}=\dot{q}_w(x) \tag{20}$$

$$\lim_{y\to\infty} I^*(x,y)=I_f^*$$

Based upon this formulation, a computer Code STAN 5 was written by Crawford and Kays in 1975, which was utilized in the present study.

4. Solution Methodology

The temperature distribution or heat flux along the interfacing flat plate is initially unknown. There, we impose the heat flux continuity condition given by

$$\int_0^1 -k\left(\frac{\partial\theta}{\partial Y}\right)_{w,1} dX=\int_0^1 -k\left(\frac{\partial\theta}{\partial Y}\right)_{w,2} dX \tag{21}$$

where subscripts 1 and 2 denote lower and upper surfaces of the interfacing wall, respectively.

In this step, an assumption is made, for simplicity, that the partitioning wall is infinitely thin. Then, the equation (21) can be localized as

$$\left(\frac{\partial\theta}{\partial Y}\right)_{w,1}=\left(\frac{\partial\theta}{\partial Y}\right)_{w,2} \tag{22}$$

The thermal matching between the two convective systems was achieved by an iterative process. The procedure begins by solving the natural convection problem with an appropriate initial guess on the temperature distribution in the normal direction along the same surface. The temperature gradient along the interfacing surface is then obtained from this solution, which is used, in turn, as the Neumann boundary condition for the external boundary layer. The turbulent boundary layer solution now yields the temperature distribution at the interfacing surface. This is used again for the start of a new iteration cycle. When the computed values from two adjacent iteration cycles are close enough, i.e., up to 10^{-5} for all cases, we terminate the iteration loop.

5. Results and Discussions

The heat transfer quantity of prime interest in the present problem is the overall rate of heat transfer through the cavity from the bottom to the partitioning wall. The overall Nusselt number is defined by

$$Nu=\frac{Q}{k(T_h-T_f)}=\int_0^1\left(\frac{\partial\theta}{\partial Y}\right)_w dX \tag{23}$$

Whereas the local Nusselt number is given by

$$Nu_x=\frac{h_x\Delta X}{k}=\left(\frac{\partial\theta}{\partial Y}\right)_w \Delta X/\theta_w \tag{24}$$

In the rectangular cauity region, we will present the temperature distribution along the interface wall as well as the contours of constant temperature, stream function, and vorticity in the cavity. We fixed the Prandtl number at the value of the air, 0.708, while the Grashof number was varied to four different values, which were all in the range of laminar natural convection. In addition, we considered several different values of aspect ratio to study the geometrical influence on the cavity heat transfer. The Reynolds number in the external flow, defined by $Re_f=U_fL/\nu$, was varied in the range from 6.4×10^4 to 5.1×10^5. Here, we have taken the leading distance D of the hydraulic boundary layer as, say, three times of the width of the rectangular cavity. For the purpose of specific numbering, we selected $D=$ 0.3m, for convinience. In this case, the hydraulic boundary layer above the cavity becomes turbulent.

To estabilish the overall validity of the present computaion in the cavity region, we carried out sample calculations. The test problem is a rectangular cavity with bottom and upper walls insulated and side walls differentially heated, which was treated previously by Cormack *et. al.*(13). In Fig. 2, results are presented in the form of streamlines, isotherms and vorticity contours. As observed, these results offer good agreement between the two sets of data. We now present the computational results for the title problems hereafter.

For aspect ratio $A=1$, variation is made in the parameter Gr_L, the Grashof number. In Figs. 3 (1) and 3 (2), as Grashof number is increased from 2×10^4 to as high as 10^6, the cavity vortex is remarkably devided into twin

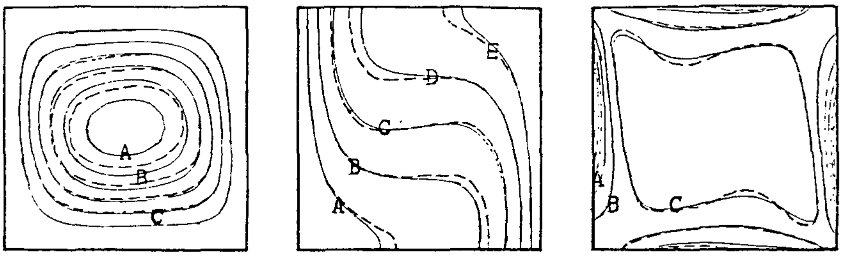

Fig. 2 Results of test-calculation ($Gr_L=2\times10^4$, $Pr=0.733$, $A=1$)
Left : streamlines ($A=3.92\times10^{-4}$, $B=2.62\times10^{-4}$, $C=1.31\times10^{-4}$)
Middle : isotherms ($A=0.167$, $B=0.333$, $D=0.667$, $E=0.833$)
Right : vorticit contours ($A=-1.41\times10^{-2}$, $B=-5.77\times10^{-3}$, $C=2.55\times10^{-3}$)
——— : Present, ... : Cormack *et. al.*(13)

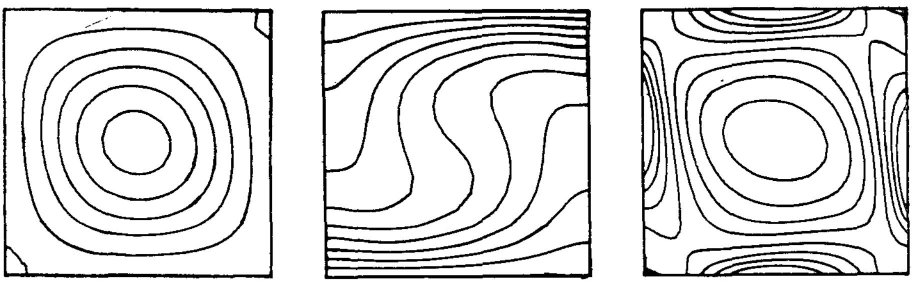

(a) Streamlines (b) Isotherms (c) Vorticity contour

Fig. 3(1) Externally-blown rectangular cavity ($Gr_L=2\times10^4$, $Re_f=6.4\times10^4$, $A=1$)

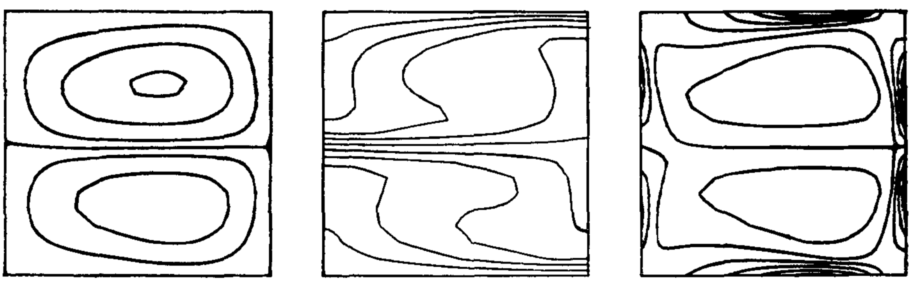

(a) Streamlines (b) Isotherms (c) Vorticity contour

Fig. 3(2) Externally-blown rectangular cavity ($Gr_L=10^6$, $A=1$, $Re_f=6.4\times10^4$)

cells, one on the top of the other. Multiple cells have been known to play an important role in transferring large amount of heat flux through the cavity for the given range of Grashof number before the convection is turned into a violent stage. From the vorticity contour distribution in Fig. 3(1), we note that the viscous friction is large near the center of each side wall, and convection is dominant in the core region.

A rectangular cavity with aspect ratio $A=0.5$ is considered next. Figure 4(1) represents a cavity flow without the external boundary layer on the top wall, while Fig. 4(2) corresponds to the same case but with external blowing at $Re_f=6.4\times10^4$. It is evident that the pattern of convection in the cavity is completely changed for a fixed Grashof number depending on the existence of the external blowing: the single cell in th cavity is multiplied as the external blowing is initiated.

For a lower aspect ratio of the cavity, say $A=0.25$, the cellularization of the cavity flow becomes more distinguished as seen in Fig. 5 (1) and 5(2). The tendency toward multiple cells is clearly stronger for the higher Grashof number. In Fig. 5(1) we see two pairs of twin vortices, and three pairs in Fig. 5(2). These

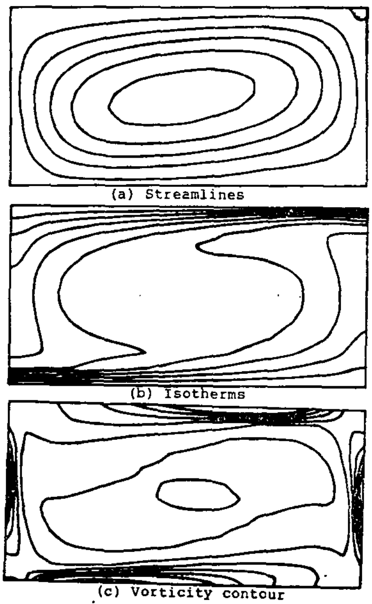

Fig. 4(1) Rectangular cavity without external blowing ($Gr_L=5\times10^6$, $A=0.5$)

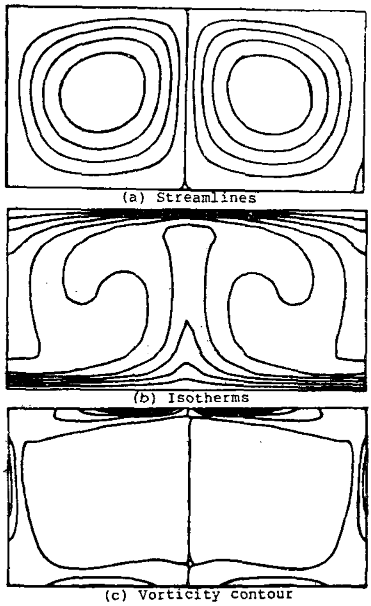

Fig. 4(2) Externally-blown rectangular cavity ($Gr_L=5\times10^6$, $A=0.5$, $Re_f=6.4\times10^4$)

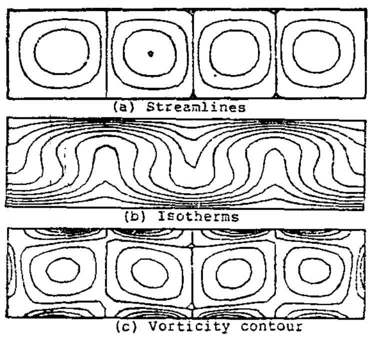

Fig. 5(1) Externally-blown rectangular cavity ($Gr_L=10^6$, $A=0.25$, $Re_f=6.4\times10^4$)

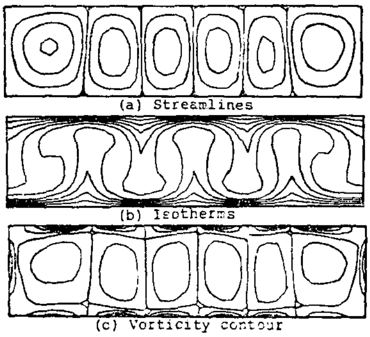

Fig. 5(2) Externally-blown rectangular cavity ($Gr_L=10^7$, $A=0.25$, $Re_f=6.4\times10^4$)

multiple cells contribute to larger heat transfer through the cavity, since the local heat transfer along the interface wall experiences multiple peaks, as will be shown shortly.

It is worthwhile to indicate the rotational direction of the cavity vortex cells. Without exception, it is observed that for a rectangular cavity externally blown on the top, the first cell in the leeward direction rotates in the direction same as an open cavity externally blown. This is the fact that heat transfer is increasing in the leeward direction while the bottom wall of the cavity remains constant in its temperature. This seems to be one of the most peculiar effects of external blowing on the internal cavity flow.

Figure 6 represents the wall temperature distribution along the interface wall. Higher Reynolds number in the external flow means lower wall temperature along the interface. The magnitude of the local wall temperature for the case $Re_f=5.1\times10^5$ is slightly less than half of that for $Re_f=6.3\times10^4$.

In Figs. 7(1) and 7(2), we plotted the local Nusselt number distribution along the interface wall for a cavity of aspect ratio $A=0.25$. Higher Reynolds number in the external flow causes higher local Nusselt number in all the cases of Grashof number considered. For higher Grashof number, the magnitude of local Nusselt number is seen decreased due to the fact that, in its definition given by Eq. (24), the denominator θ_w grows faster than the numerator $(\partial\theta/\partial Y)_w$ as the Gr_L is increased.

It is noted in these figures that the magnitude of the peak values in the local Nusselt number increases leeward, which is possibly due to the increased turbulence intensity in the stream direction of the external boundary layer.

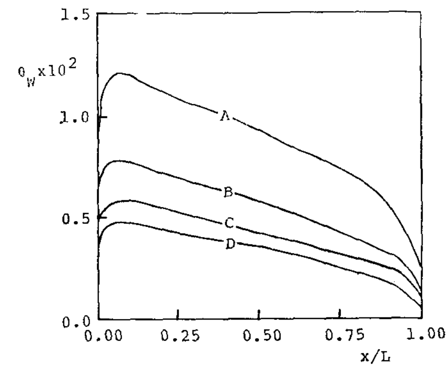

Fig. 6 Tomperature distribution at the interface wall($Gr_L=10^6$, $A=1$). Reynolds number Re_f : $A=6.4\times10^4$ $B=1.3\times10^5$, $C=2.6\times10^5$, $D=5.1\times10^5$

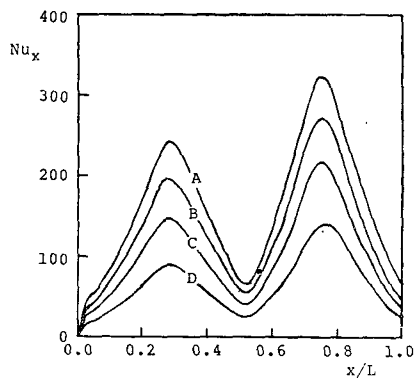

Fig. 7(1) Local Nusselt number along the interface wall($Gr_L=10^6$, $A=0.15$). Reynolds number Re_f : $A=5.1\times10^5$, $B=2.6\times10^5$, $C=1.3\times10^5$, $D=6.4\times10^4$

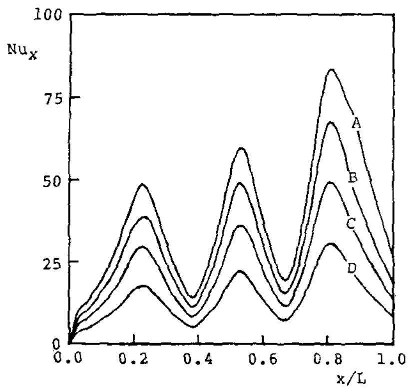

Fig. 7(2) Local Nusselt number along the interface wall ($Gr_L=5\times10^6$, $A=0.25$). Reynolds number Re_f : $A=5.1\times10^5$, $B=2.6\times10^5$, $C=1.3\times10^5$, $D=6.4\times10^4$

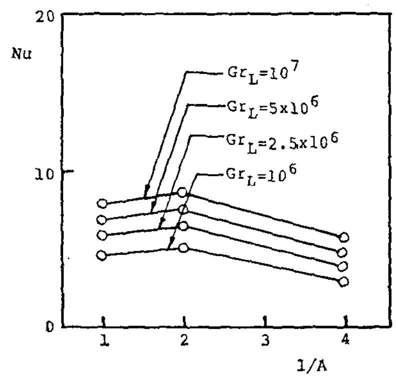

Fig. 8 Overall Nusselt number as a function of aspect ratio ($Re_f=6.4\times10^4$)

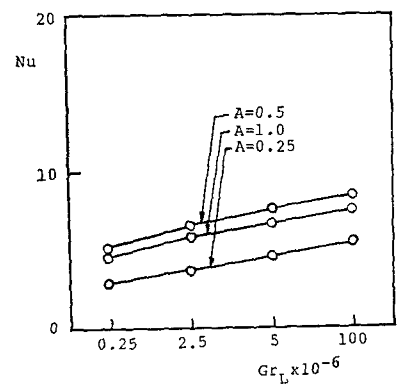

Fig. 9 Overall Nusselt number as a function of Grashof number($Re_f=6.4\times10^4$)

Finally, the overall Nusselt number for the cavity flow is plotted in Fig. 8 and 9. It is clear that there exists an optimal aspect ratio for which the overall Nusselt number becomes maximum at fixed Grashof number and Reynolds number of external blowing. This value of optimal aspect ratio is located roughly near 0.5 for $Re_f=6.4\times10^4$ as seen in both Fig. 8 and 9. The rather linear dependence of the overall Nusselt number on the Grashof number is observed in Fig. 9 for all the aspect ratios considered.

6. Conclusions

The results obtained from the conjugate natural-to-forced convection heat transfer suggest following facts.

(1) The flow parameters responsible for the detailed convection pattern in the cavity are the Grashof number and the Reynolds number of the external boundary layer. The wall heat flux and the cellularity of the cavity flows are directly influenced by them.

(2) The rotation of the cavity vortices is dictated by the existence of the external blowing. The first cell in the leeward direction always rotates in the direction same as an open cavity flow externally blown.

(3) For a fixed Grashof number, an optimum aspect ratio which maximize the overall heat transfer rate exists.

(4) For low aspect-ratio rectangular cavity, the number of vortex cells are increase in an even number as the Grashof number is increased.

(5) The peak local Nusselt number at the interface wall increases in its magnitude in the leeward direction possibly due to the enhanced streamwise turbulent convection in the external boundary layer.

References

(1) H.L. Kuo, "Solution of the non-linear equations of cellular convection and heat transport," J, Fluid Mech. Vol. 10, pp. 611~634, 1961

(2) A. Cabelli and G. De Vahl Davis, "A numerical study of the Benard cell," J. Fluid Mech. Vol. 45, part 4, pp. 805~829, 1971

(3) M.R. Samuels and S.W. Churchill, "Stability of a fluid in a rectangular region heated from below," AICHE Journal, Vol. 13, No. 1, pp. 77~85, 1967

(4) J.E. Deardorff, J. Atmos. Sci. 21, pp. 419, 1964

(5) J.E. Fromm, "Numercal solution of the nonlinear equations for a heated fluid layer", Physics of Fluid, Vol. 8, No. 10, pp. 1757~1769, 1965

(6) K. Küblbeck, G. P. Merker and J. Straub, "Advanced numerical computation of two dimensional time dependent free convection in cavities", Int. J. Heat and Mass Transfer, Vol. 23 pp. 203~217, 1980

(7) B.A. Meyer, J. W. Mitchell and M. M. El-Wakil, "The effect of thermal wall property on natural convection in inclined rectangutar cells", ASME J. Heat Transfer, Vol. 104, pp. 114~117, 1982

(8) S.M. ElSherbiny, K.G.T. Hollands and G.D. Raithby, "Effect of thermal boundary conditions on natural convection in vertical and inclined air layers", ASME J. Heat Transfer, Vol. 104, pp. 515~520, 1982

(9) R.A. Wirtz, J. Righi and F. Zirilli, "Measurements of natural convection across titled rectangular enclosures of aspect ratio 0.1 and 0.2", ASME J. Heat Transfer, Vol. 104, pp. 521~526, 1982

(10) Patankar and D.B. Spalding, "A finite difference procedure for solving the equations of two dimensional boundary layer", Int. J. Heat and Mass Transfer, Vol. 10, pp. 1389~1411, 1967

(11) M.E. Crawford and W.M. Kays, Report HMT-23, NASA NGR-05-020-134 NAS 3-14336, 1975

(12) G.S.M. Lock and R.S. Ko, "Coupling through a wall between two free convective systems", Int. J. Heat and Mass Transfer, Vol. 16, pp. 2087~2096, 1973

(13) D.E. Cormack, L.G. Leal and J.H. Seinfeld, "Natural convection in a shallow cavity with differentially heated end walls", J. Fluid Mech. Vol. 65, part 2, pp. 231~246, 1974

(14) D.K. Lilly, "On the computational stability of numerical solution of time-dependent nonlinear geophysical fluid dynamics problems", Monthly Weather Rev. 93(1), pp. 11~26, 1965